Fully 3D Printed Flexible, Conformal and Multi-directional Tactile Sensor with Integrated Biomimetic and Auxetic Structure

Yuyang Wei
The University of Manchester https://orcid.org/0000-0002-3200-8598
Bingqian Li
Jilin University
Marco Domingos
University of Manchester https://orcid.org/0000-0002-6693-790X
Yiming Zhu
The University of Manchester
Lingyun Yan
The University of Manchester https://orcid.org/0000-0002-9986-2182
Lei Ren (lei.ren@manchester.ac.uk)
University of Manchester
Guowu Wei
University of Salford https://orcid.org/0000-0003-2613-902X

Article

Keywords: tactile sensors, 3D printing, biomimetics

Posted Date: September 20th, 2021

DOI: https://doi.org/10.21203/rs.3.rs-877986/v1

Fully 3D Printed Flexible, Conformal and Multi-directional Tactile Sensor with Integrated Biomimetic and Auxetic Structure

Author Information

Affiliations

[1]School of Mechanical, Aerospace and Civil Engineering, The University of Manchester, Manchester, UK

[2]Key Laboratory of Bionic Engineering, Ministry of Education, Jilin University, China

[3]The Institute of Mechanical Engineering, University of Salford, Manchester, UK

Yuyang Wei-1, Bingqian Li-2, Marco Domingos-1, Yiming Zhu-1, Lingyun Yan-1, Lei Ren*-1,2 and Guowu Wei*-3

Contributions

YW designed, fabricated the sensor, performed the experiments, analyzed the data, and wrote the paper. MD helped to revise the paper and give advice. BL, YZ and LY performed some experiments. LR and GW supervised the whole research and analyzed the data.

Corresponding author

Lei Ren* and Guowu Wei*, Email: lei.ren@manchester.ac.uk or g.wei@salford.ac.uk

Abstract

Tactile sensors are instrumental for developing the next generation of biologically inspired robotic prostheses with tactile feedback. Despite significant advancements made in current sensing technology, several limitations still exist including the reduced sensing sensitivity under high pressure, lack of compliance of the planar sensor with working surfaces and the demand for sophisticated manufacturing processes. In this study, we investigate the feasibility of using the 3D printing technology for the rapid and simple fabrication of a new conformal tactile sensor with an improved linear sensing range. The auxetic structure is integrated with a biomimetic inter-locked papilla feature which allows to detect multi-directional stimuli. Using the proposed design, the linear sensing range is extended to 0.5MPa and responsive to normal and shear forces with the sensitivities of 2.42KPa^{-1}and 2.20N^{-1} respectively. The proposed tactile sensor was printed on the fingertip of a prosthetic robotic hand to perform the sensorimotor control, or on the proximal femur head and lumbar vertebra for monitoring the bone-on-bone load. The results have shown promising application prospects of the proposed tactile sensor.

Introduction

Over the past decade, great attention has been dedicated to the development of wearable, flexible tactile sensors or electronic skin for applications in prosthetics, robotics and healthcare monitoring devices [1-11]. Independent of applications, tactile sensors should be able to detect multi-directional stimuli, and for that purpose different strategies have been proposed including the use of advanced composite materials, multi-layered biomimetic or hierarchical structures [6,10-13]. Complex manufacturing approaches such as molding, photolithography and etching technologies are traditionally employed in the fabrication of high-performance sensors [14-17] and often require sophisticated methods for the preparation of the materials. Most of the existing tactile sensors have a planar structure which does not allow for optimal fixation on uneven working surfaces, thus limiting their range of applications. To exploit the full potential of sensing technology and deliver the next generation of prosthetics, alternative strategies must be developed,

enabling high performance tactile sensors with more complex structures to be rapidly manufactured at feasible costs.

In an attempt to improve the sensitivity and linear sensing range of tactile sensors, different researchers have reported the combination of highly conductive composite materials such as metallic particles, nanowires [6], carbon nanotubes (CNT) [18], graphene palate [19] with an insulation matrix. Microspheres can also be integrated with nanomaterials, forming hierarchical structures with enhanced piezoresistive properties [12,13,19-22]. Carbon nanotubes (CNT)/polymer composites have also been widely exploited in the generation of dielectric layers due to their high axial conductivity. When compared to similar quantities of carbon black or graphene, the addition of CNTs to polymer matrices can induce a substantiality higher piezoresistive response with minimal effect on the mechanical properties of the composite [23-25]. Volatile or water soluble micro-particles were also employed by researchers to generate sponges or porous material [8,19], increasing the self-contact area and linear sensing range. However, the process for producing these multiscale and hierarchical materials is time-consuming and technically complicated [20]. The stability and homogeneity of the material cannot be precisely controlled thus affecting the final structure and performance of the sensor. In particular, the sensitivity and linear sensing range, can be improved through the use of porous or hollow structures [8,18,19], multiscale hierarchical structures [5,6,20], biomimetic interlocked structures [11,22,26,27], mechanosensory hair or even crack like structures [28,29]. In a recent study, Park et al. has reported the fabrication of a series of interlocked micro-dome arrays capable of amplifying the signal response whilst differentiating between multiple stimuli directions [10,11,20]. With the same goal in mind, other researchers have used multilayer or hierarchical hair-like interlocked geometries [6,9] to push the boundaries of sensitivity and obtain an extra low detection threshold of 0.6 Pa. However, these structural features need a sophisticated and time-consuming fabricating process. The enhanced performance reported in these studies still does not translate into a wider use of sensing technology. One of the reasons may be related to the complexity of the manufacturing processes and associated costs, still prohibitive for many research groups and industries [14-17]. The use of advanced composite materials could

be seen as an alternative to the above strategies, but the long production time and high-demanding operating environments are limiting factors when considering their use at industrial scale. Another important issue that remains unsolved is the generation of a strong, stable and durable interface between the sensor and the working surface [26,30].

In this paper, we propose a new approach based on the use of 3D printing technology and advanced materials to fabricate a biomimetic tactile sensor, which can detect both normal and shear forces. The 6 by 6 flexible tactile sensor (Fig. 1a) can be printed directly onto any uneven surfaces, such as the fingertip of a biomimetic hand for sensorimotor control, or the vertebra and femur for bone-on-bone load monitoring. When compared with other tactile sensors made of similar piezoresistive material, the integrated biomimetic inter-locked and auxetic structure (Fig. 1b) of the proposed sensor lead to improved performance at different levels, namely: 1) higher sensitivity to strain variations; 2) larger linear sensing range and sensitivity due to negative Poisson's ratio; 3) easy detection of stimuli direction. More than simply overcoming the limitations of the current technology, this study aims to provide new tools towards the design and fabrication of pressure sensors with user-defined auxetic features tailored for specific applications.

Results

The structure design and 3D printing of the tactile sensor

The proposed tactile sensor array was fully 3D printed containing the upper and lower papilla-auxetic dielectric layer sandwiched between two flexible electrode layers. Fig. 1a-e present the layout of the flexible tactile sensor array consisting of 36 sensing elements ($2 \times 2mm^2$ for each sensing element). The sensing area for each element is similar to the receptive filed of the slowly adapting type I (SAI) mechanoreceptor 31 to ensure a close match between the sensing capability of our sensor and that of the human subject. The biomimetic inter-lock structure was integrated to enhance the sensitivity and differentiating the directions of the external stimuli. Our results show that piezoresistive sensing elements (located at the position of each small papilla) placed on the side of the applied force experienced

substantially larger pressure and reduction of resistance compared to those placed on the opposite side. This can be associated with the geometric features of the lower large papilla and the anisotropic deformation of the upper dielectric layer with small papilla. The direction of the shear force could be intuitively differentiate based on each large papilla (Fig. 1f), surrounded by four small papillae above its four corners. The two small papillae on the side of the shear force experienced larger current increments than the other two on the opposite side. Therefore, the pressure mapping on the tactile sensor array, originated by the anisotropic distribution of resistance around the lower papilla, provided the ability to detect and differentiate between shear forces with different directions (four in total). On the other hand, the single sensing element was not able to provide the bulk information on force direction.

A CNT-Silicon rubber composite was used as the printing material for fabricating this high-performance tactile sensor. The multi-wall CNT was evenly distributed within the silicon matrix (Fig. 2a), providing piezoresistive properties under external stimuli. The conductive micro-copper-silicone composite was employed to print the electrode, more detailed information on its preparation can be found under materials and methods section. Printability of developed composite materials was determined through rheological measurements, in particular by measuring the variation of viscosity and shear stress as a function of shear rate (see Supplementary Fig. 1 and 2). The viscosities of both composites were decreasing under shear strain during amplitude sweep test which means these composites could be used as 3D printing materials in terms of the rheology properties.

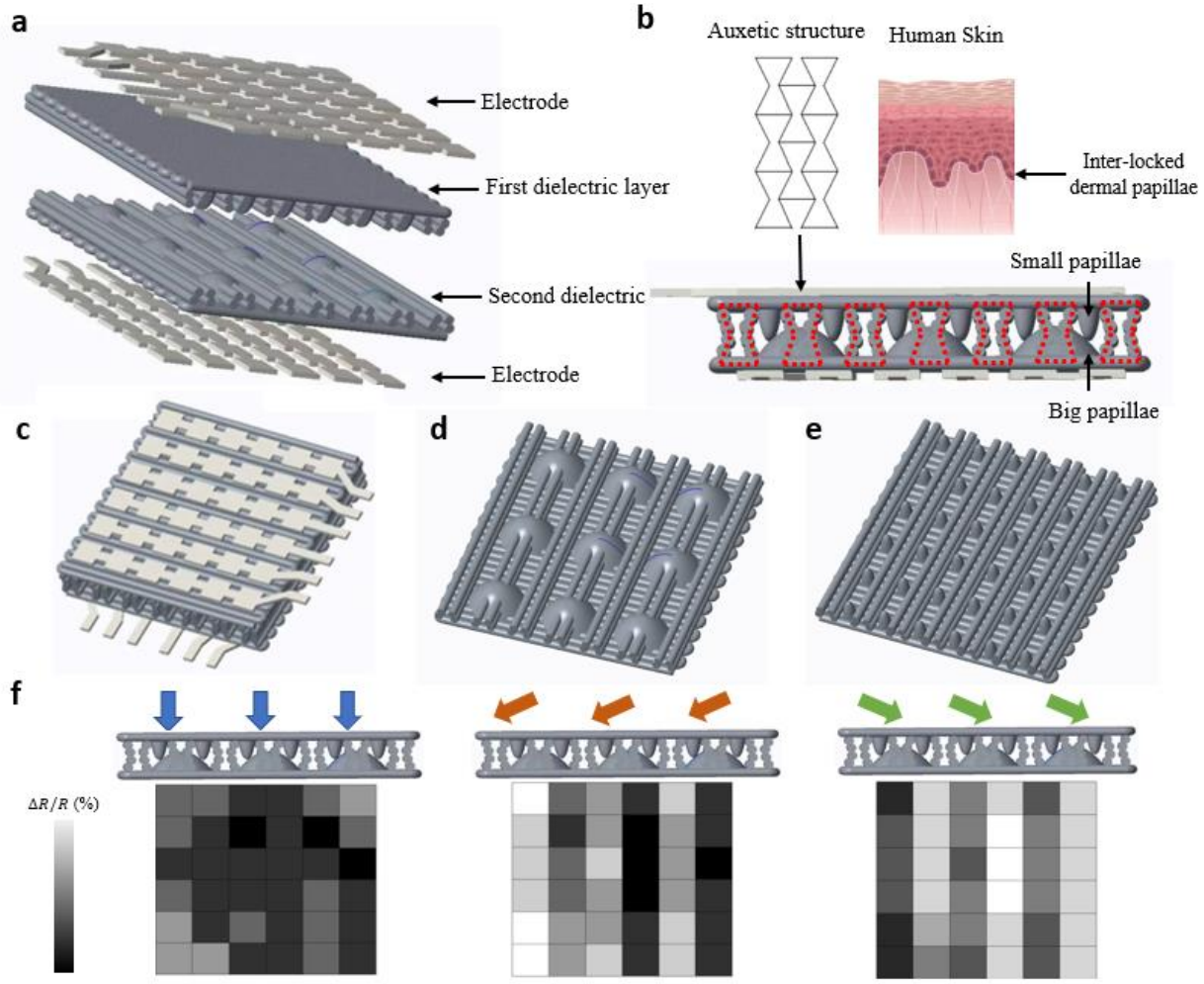

Fig.1 The structure and working principle of the tactile sensor. (**a**). A standard 6×6 tactile sensor array. Each sensing element corresponds to a small papilla of the inter-locked structure. (**b**). The integrated auxetic and biomimetic inter-locked structure of the sensor. The auxetic structure is highlighted in red dash line, the small and large papilla are located on upper and lower dielectric layer, respectively. (**c**) The 3D model of the sensor. The sensor is composed by a dielectric layer sandwiched between two layers of electrodes. (**d**) The lower dielectric layer of the sensor consists of nine large papilla structures and auxetic lines. (**e**). The upper layer of the sensor consists of 36 small papilla structures and auxetic lines. (**f**) The stimuli are applied from different directions (indicated by the arrows above the sensor) and the corresponding pressure distribution shown through a customized graphical user-interface (GUI).

In order to print the electrode and dielectric layer, the composite material was loaded into a syringe and transferred to the multi-material 3D printer developed in house (Fig. 2 d to g). Afterwards, the double layered sensor, comprising an upper and lower papilla-auxetic structures and containing the electrodes, was directly fabricated according to the G codes developed manually based on the 3D models. The moving speed ranging from 5 to 15mm/s (step increment 1mm/s) under the pressure varied from 0.5 to

1.5 bar (step increment 0.1bar) were used to carry out the trail line printing, resulting in totally 121 different combinations of printing parameters. The pressure of 0.7 bar with printing speed of 12mm/s was found achieving a stable printing quality and appropriate extrusion width. The pressure of 1 bar was set for dot-printing the papilla structure.

Firstly, the electrode was directly written with a 15-gauge needle mounted on the syringe loaded with silver coated copper-silicone composite material. Another syringe with the CNT-silicone composite was replaced and mounted with 22-gauge needle for line printing auxetic structure of the lower dielectric layer. A 10-gauge needle was then changed for dot printing the large papilla structure on top of the lower layer. Similar printing parameters and patterns were applied for printing the upper papilla-auxetic structure. Finally, the upper electrode was printed on top of the sensor. The working surface for printing the sensor was discretized with a fine mesh in commercial FE software Abaqus (Dassault Systèmes Simulia Corp., UK). The coordinates of the nodes were transferred to G code for printing in order to obtain a good compliance between the printed path and the target surface. The printing process of the sensor is shown in Movie 1.

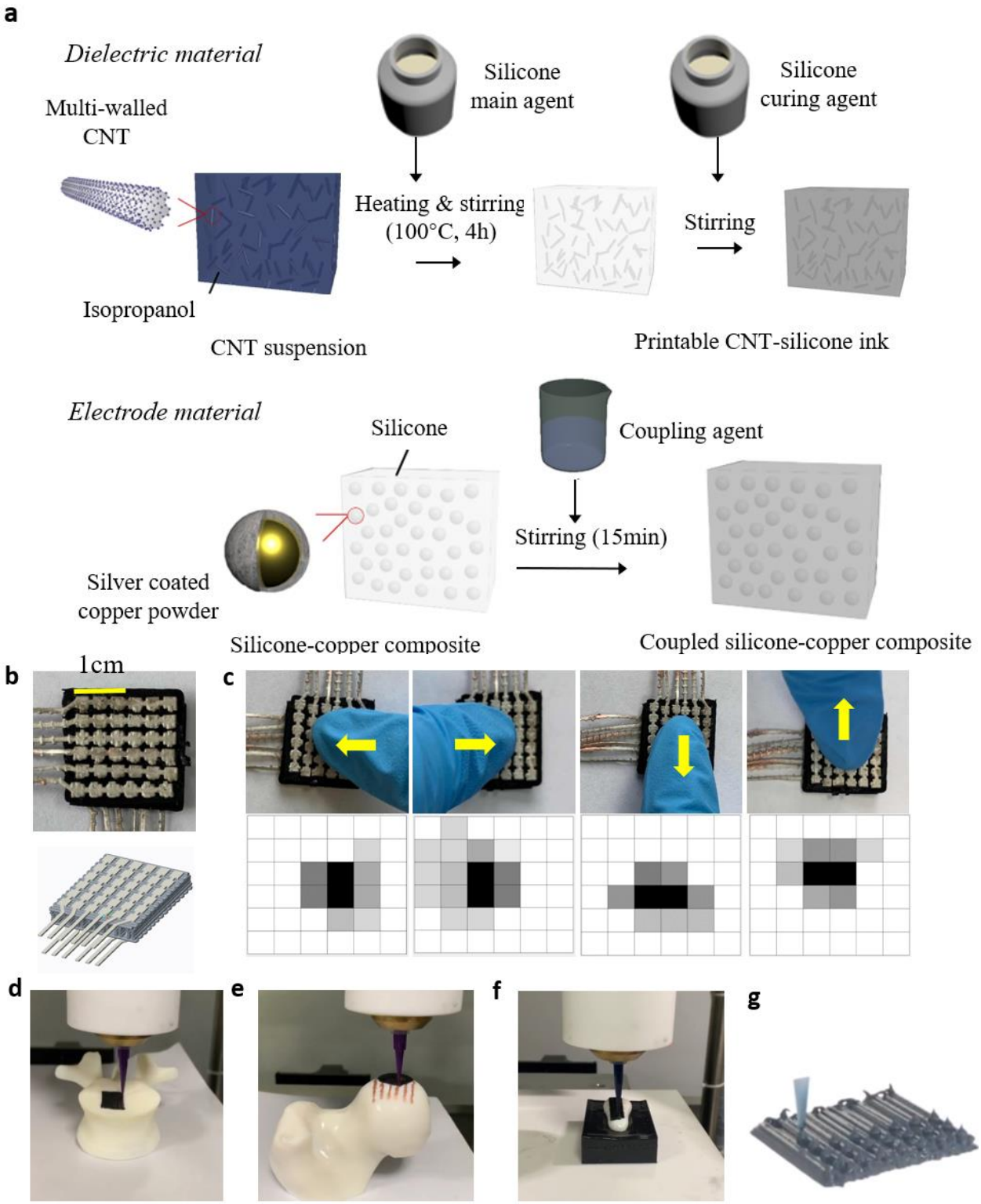

Fig.2. The material preparation and 3D printing of the sensor. (**a**) The material preparation of the silicone-CNT and silicone-copper composite (**b**) The physical prototype and 3D model of the printed sensor. (**c**) The fingertip contact force was applied on tactile sensor, the direction of the shear force was indicated by the arrows in yellow. The distribution of the contact pressure are shown through customized graphic user-interface, it can be seen that the sensing elements on the sides of the shear force experienced

larger resistance variation. (**D**) The 3D printed sensor on a model of human vertebra. (**E**) The 3D printed sensor on the proximal femur head. (**F**) The 3D printed sensor on the distal index phalange. (**G**) The 'dot printing' for inter-locked papilla structure.

Auxetic structure optimization of the tactile sensor

Research has shown that the auxetic structure can provide negative Poisson's ratio and larger self-contact area 32. Therefore, the auxetic structure was applied to enlarge the linear sensing range and enhance the sensitivity. The thickness and re-entrant angle of the auxetic structure (Fig. 3a and b) was optimized to achieve the best nominal sensitivity and the predicted results were also validated against couple of experiments (Fig. 3b and c). The sensitivity (S) of the piezoresistive pressure sensor was defined as

$$S= (\Delta I/I0)/\Delta P \quad (1)$$

in the linear regime, where I is the current flow over the dielectric layers and P is the applied pressure.

The nominal sensitivity (Sn) for optimizing the auxetic structure was defined as

$$Sn= (\Delta SED/SED0)/\Delta P \quad (2)$$

Where SED stands for the strain energy density at the site of the sensing elements.

Research on piezoresistive characteristics of the elastic polymer-based sensor has shown that the sensitivity is dominated by the geometry of the structure and the stress/strain experienced within the composite 33-35. Due to the relatively small variations in the geometry of thin film-like flexible sensors, the change of strain energy density relative to the external pressure was considered as the main factor affecting the piezoresistive effect. Therefore, the variation of SED was employed instead of current for evaluating the nominal sensitivity. The structural parameters (Fig. 3a) to be optimized were re-entrant angle (from 45° to 90° with the increment of 1°) and H/L (Fig. 2b) ratio (H/L=2.7, 2.0, 1.6 1.3 1.0). Totally 230 trails of simulation were performed in commercial FE software Abaqus. The sensor with re-entrant angle of 65° and the H/L ratio of 1.60 achieved the largest nominal sensitivity according to the simulation results. Meanwhile, twenty tactile sensors with the re-entrant angle of 45°, 60°, 75°, 90° and five H/L ratios were fabricated to validate the FE simulation results for structure optimization. Fig. 2a shows the results of the optimization and validation. The transparent mesh stands for the real sensor

characterization results while the solid mesh represents the simulation results. Both the experiment and simulation results suggested that the sensitivity and linear sensing range were significantly enhanced by the integrated inter-locked and auxetic structure. The simulation results also reveal that different re-entrant angles and H/L ratios of the auxetic features can significantly affect the sensitivity of the tactile sensor. The simulation output of compression tests for the sensors with different auxetic features are available in Movie. 2.

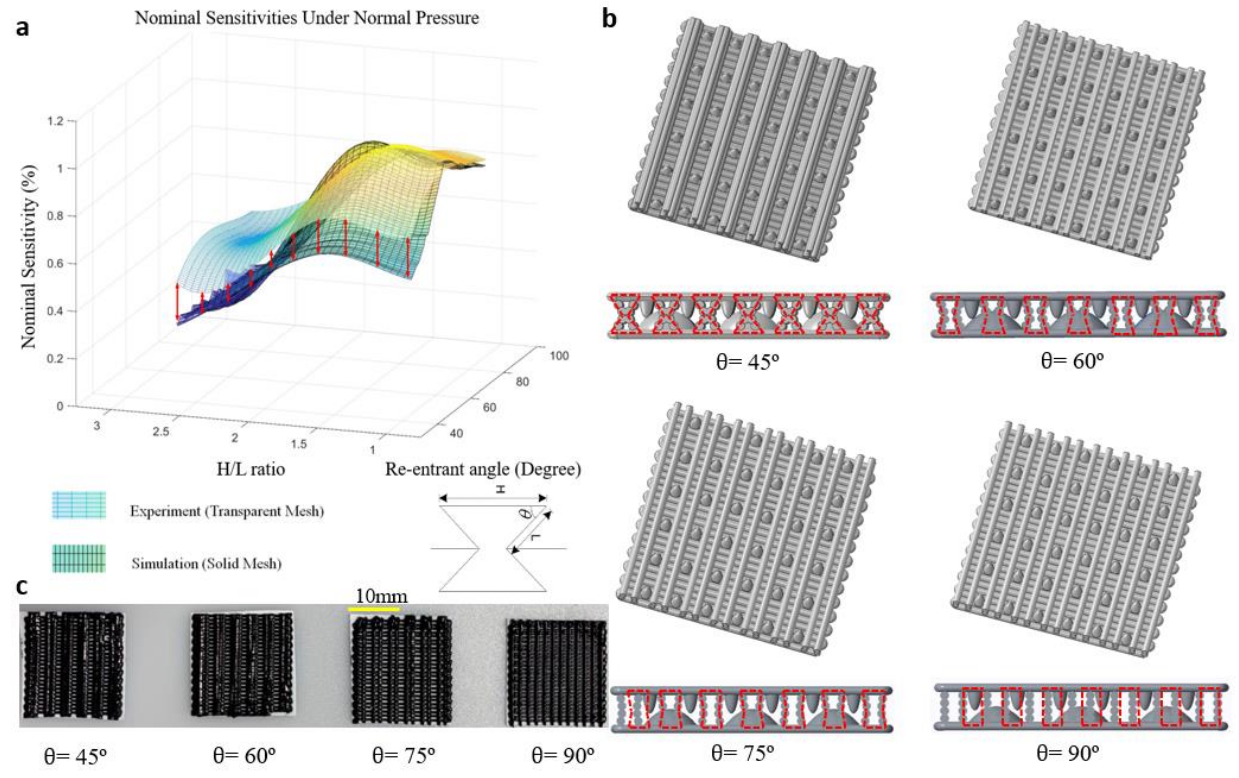

Fig. 3. The optimization results of the sensor and the prototypes with different structures. (**a**) The optimization results for the auxetic structure. The largest nominal sensitivity was achieved under the re-entrant angle of 65° and H/L ratio of 1.6. The sensor with different auxetic structures were also fabricated to validate the simulation results. The tactile sensors with re-entrant angle of 45°, 60°, 75°, 90° and H/L ratio of 1.06, 1.3, 1.6, 2.0, 2.7, totally 20 samples with different geometric parameters were fabricated. Their sensitivities were measured and compared with the predicted nominal sensitivity derived based on the simulation results. The difference between simulation and experiment results were indicated in red arrows. The nominal and the measured sensitivities agreed well with each other. (**b**) The 3D model of the sensors with four different re-entrant angles modelled for structure optimization. The auxetic structures with different re-entrant angles are highlighted in red dash lines. (**c**) The fabricated prototype of the auxetic structure of the lower dielectric layer. The re-entrant angle of 45°, 60°, 75°, 90° were presented. (**d**) The simulation results of the compression experiments for the sensors with different auxetic structures. The sensors were shown in three stages: before during and after compression. The simulation results of the sensors with re-entrant angle of 60° and different H/L ratios are presented. The sensors before, during and after the compression are shown in supplementary Fig.3.

Characterization of the sensor

Fig.4 illustrates the characterization of this high-performance tactile sensor including the sensitivity (Fig. 4a, b), linear sensing range (Fig4. a, b), the lower detection limits and the response time (Fig. 4c). The sensitivity of the sensor with three different structures were compared in Fig.4d and 4f. The sensitivity (Under the pressure below 10KPa which is the threshold pressure of gentle touch during daily living 36) of the planar sensor was below $1KPa^{-1}$ while was significantly increased to $2.42KPa^{-1}$ by integrating the interlocked papillae and optimized auxetic structure. Meanwhile the linear sensing range also increased from 0.1 MPa to 0.5 MPa, which is one order of magnitude higher compared with most of the published high-performance sensors 1-3,11,18. The inter-locked features not only provide the sensor with the ability of differentiating directions of the shear force but also improve its sensitivity. Importantly, the integration of the auxetic structure allowed for enhanced sensitivity and extended the linear sensing range. The tactile sensor was mounted onto a customized horizontal testing platform with a push-pull dynamometer to generate the shear force (from 0 to 5 N) while a universal testing machine was used to provide the normal compression force. The shear sensitivity was quantified under the normal contact pressures ranging from 0.2KPa to 10KPa, the maximum shear sensitivity of $2.26N^{-1}$ was found under the normal pressure of 0.2KPa and reduced with the increased compression force. The shear sensitivity was maintained at approximately $1.5N^{-1}$ under the compression pressure ranging from 0.4 to 0.8 KPa and

was reduced to $0.83N^{-1}$ when the normal pressure was above 1KPa. It can be found from the Fig. 4c that the shear sensitivity was significantly dominated by the inter-locked and auxetic structure of the sensor. Only $0.37N^{-1}$ of the sensitivity was achieved by the planar dielectric layer while it increased to $2.26N^{-1}$ after integrating the biomimetic and auxetic features. The lower detection limit was found to be around 10Pa as is presented in Fig. 4d, the response time is approximately 35ms recorded by the multimeter. The standard 36 sensing element tactile sensor was tested under repeated pressing and releasing cycles in a wide range of compressive deformation. The stable signal response was achieved after 2000 loading-unloading cycles.

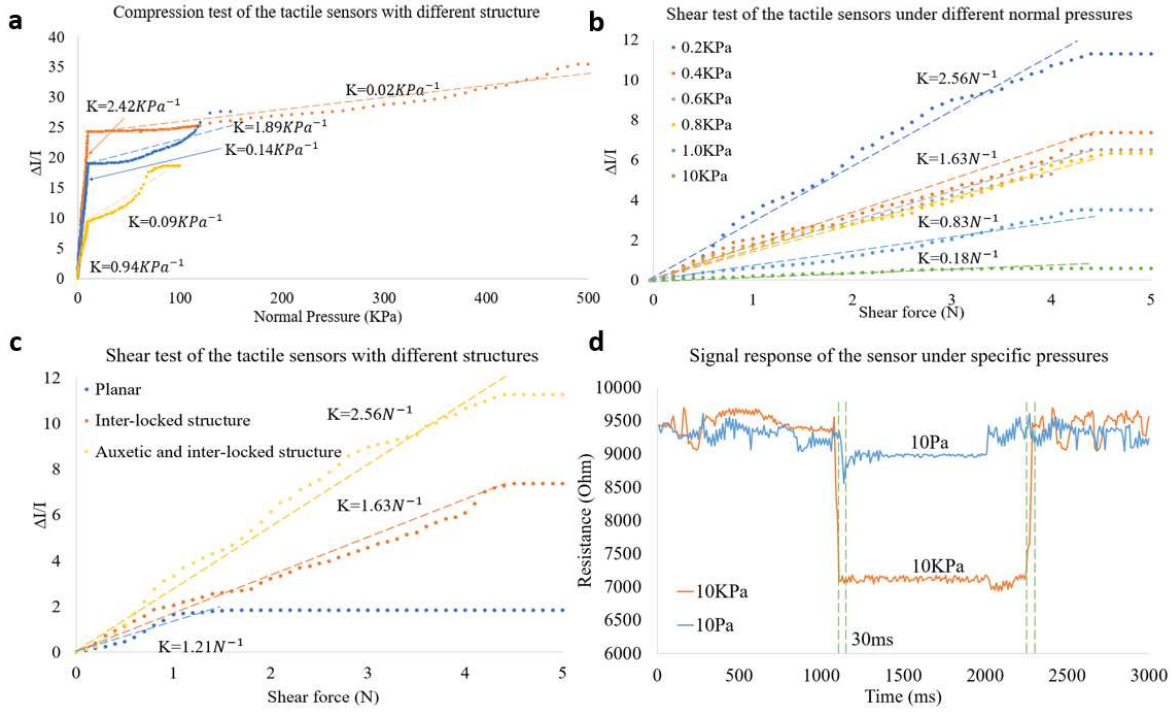

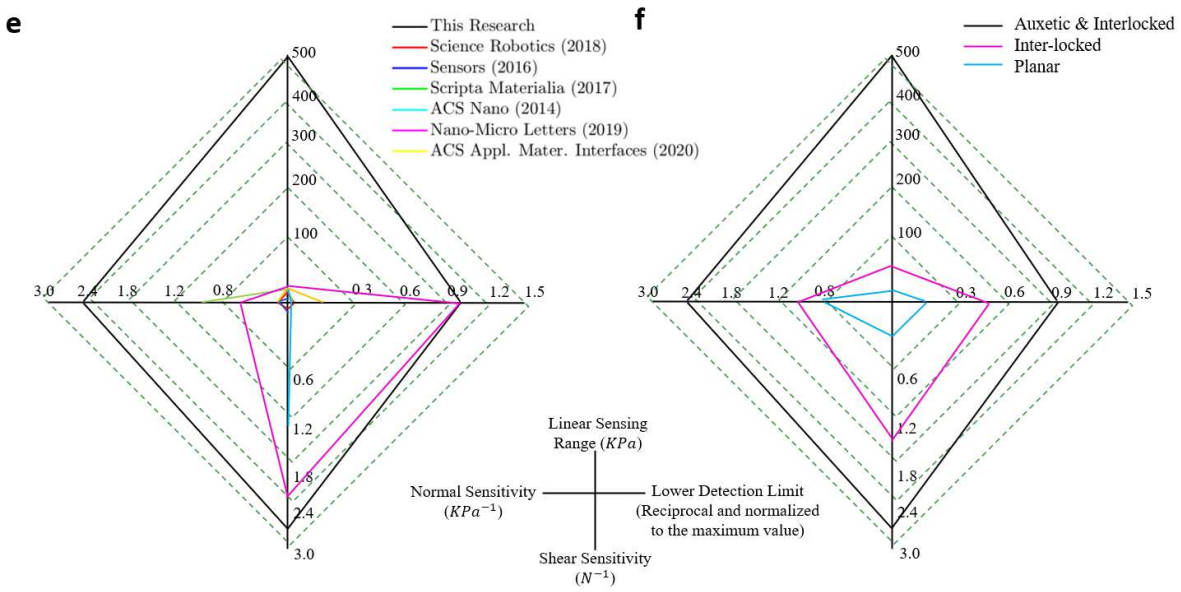

Fig. 4. The characterization and performance of the tactile sensor compared with other published sensors. (**a**). The sensitivity of the sensors with different structures including planar sensor, the sensor with the inter-locked structure and the sensor with both inter-locked and auxetic structure. The sensitivity was summarized within and beyond the 'gentle touch pressure, 10KPa'. (**b**) The shear sensitivity of the sensor under different normal pressures varied from 0.2 to 10KPa. (**c**) The signal response of the sensor under the lowest detection limit 10Pa and gentle touch pressure 10KPa. (**d**) The shear sensitivity of the sensor with three different structures. (**e**). The comparisons of sensing performance between the published sensors and the tactile sensor developed in this study. The lower detection limitations were reciprocal and then normalized to the maximum value. Therefore, a larger index of the lower detection limit in the diagram means a better sensor performance. (**f**). The comparisons of sensing performances among the planar sensor, the sensor only adopted interlocked features and the one with the integrated inter-locked and auxetic structure.

Monitoring magnitude and direction of the bone-on-bone load through the senor

This fully 3D printed tactile sensor can be directly written onto uneven working surfaces such as the human vertebra and the proximal femoral head to monitor bone-on-bone load. To demonstrate the ability of the sensor array to detect both magnitude and direction of the contact force, the sensor was directly written onto the plateau of the human vertebra and used to monitor the intervertebral compression force and torque. The L2 and L3 vertebra together with the inter-vertebra disc (Fig. 5a to 5c) were 3D printed using UV curable resin as the working surface of the sensor. The model of the L3 vertebra was discretized in Abaqus to extract the coordinates of the working surface and defining a conformal printing path of the sensor. The printed pressure sensor was wired with a customized electric circuit for collecting the analog

output from the 6 × 6 sensing elements and convert them into digital signals thus enabling visualizing on GUI interfaces (Fig. 5d). Motions of the spine including lateral bending, axial rotation and flexion/extension were performed under different compression forces ranging from 25 to 75N with grey color representing the output current and the magnitude of the pressure acting on each tactile element. The distributions of these contact patterns indicate the direction and magnitude of the forces. It can be seen from the customized GUI that the sensor performed well under the external stimuli including torque, normal and shears forces, enabling visualization of the complex contact between intervertebral disc and vertebra.

Due to the large linear sensing range, this sensor was also printed onto the proximal femoral bone to monitor the large bone-on-bone load of the hip joint (Fig. 5e). A conformal printing path around the femoral head was also defined to print the sensor. The proximal femoral head and part of the pelvis were printed to perform the kinematics of the hip joint during the swing of the lower lime. The GUI shows a reasonable pressure distribution during the whole swing phase confirming the ability of the pressure sensor to detect multi directional loads (Fig. 5f). Also, the compression test of the sensor shown in Fig. 1f and Fig. 2c present the capacity of this sensor to discriminate the directions of the stimuli based on the biomimetic inter-locked structure. Therefore, the experimental results reported above suggest that this 3D printed sensor can be rapidly fabricated onto geometrically complex surfaces such as the vertebra or femoral head and used for monitoring the magnitude and direction of the external load. The printed sensors working on hip joint and between the lumber vertebrae are presented in Movie. 3.

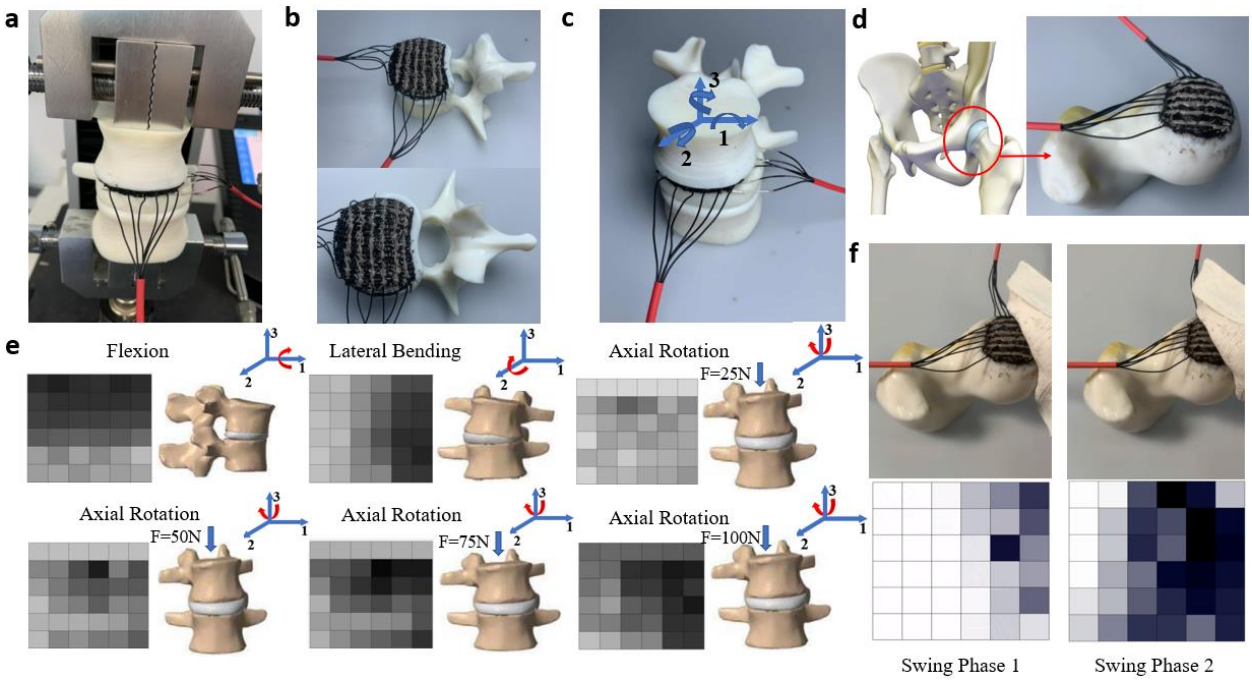

Fig. 5. The applications of the sensor on monitoring the bone-on-bone load. (**a**) The sensor was printed onto the vertebra plateau to monitoring normal compression force. (**b**)(**c**) The printed sensor onto the vertebra plateau and the rotation around three axes corresponding to flexion/extension (axis 1), lateral bending (axis 2) and axial rotation (axis 3). (**d**) The printed sensor on the distal femur bone of the human hip joint. (**e**) The signal distribution of the sensor under different motions of the spine vertebra including flexion, lateral abending and axial rotation. The axial rotation was combined with different compression force of 25, 50, 75, 100N to show the sensor performance under different combinations of loading conditions. (**f**) The signal distribution of the sensor during the swing of hip joint.

Sensorimotor control of the biomimetic hand through the tactile sensor

The 6 by 5 tactile sensor array with approximate dimensions of 15×12 mm2 was fully 3D printed onto the distal phalange of the biomimetic hand. The tendon-driven biomimetic hand employed in this study was reconstructed from a male subject, including the intact bone skeleton, tendon, interphalangeal ligaments and skin. Five motors were used to pull the tendon and achieved human like kinematics and grasping quality. The distal phalange of the index was disassembled from the biomimetic hand to print the sensor on it. A customized electric circuit was constructed to collect the analog output from the tactile sensing elements. A Python based controlling algorithm was developed to convert sensor analog output to digital signals as feedback for controlling the motors and producing contraction of the tendon. Detailed information about the hardware and controlling are illustrated in 'Materials and Methods' section.

A plastic sphere was grasped by the biomimetic hand while a 0.75N pulling force was randomly applied to provide the shear force. The tactile sensor was able to perceive the shear or slipping force on the fingertip and form a sensorimotor closed loop control to maintain the stable grasp. Fig. 6a and Movie. 4 show the reaction control of the biomimetic hand with the tactile feedback. Taken together, these results clearly show the potential of the high-performance tactile sensor to monitor magnitude and direction of stimuli, whilst providing feedback control of robotics by fast direct writing onto the target surfaces.

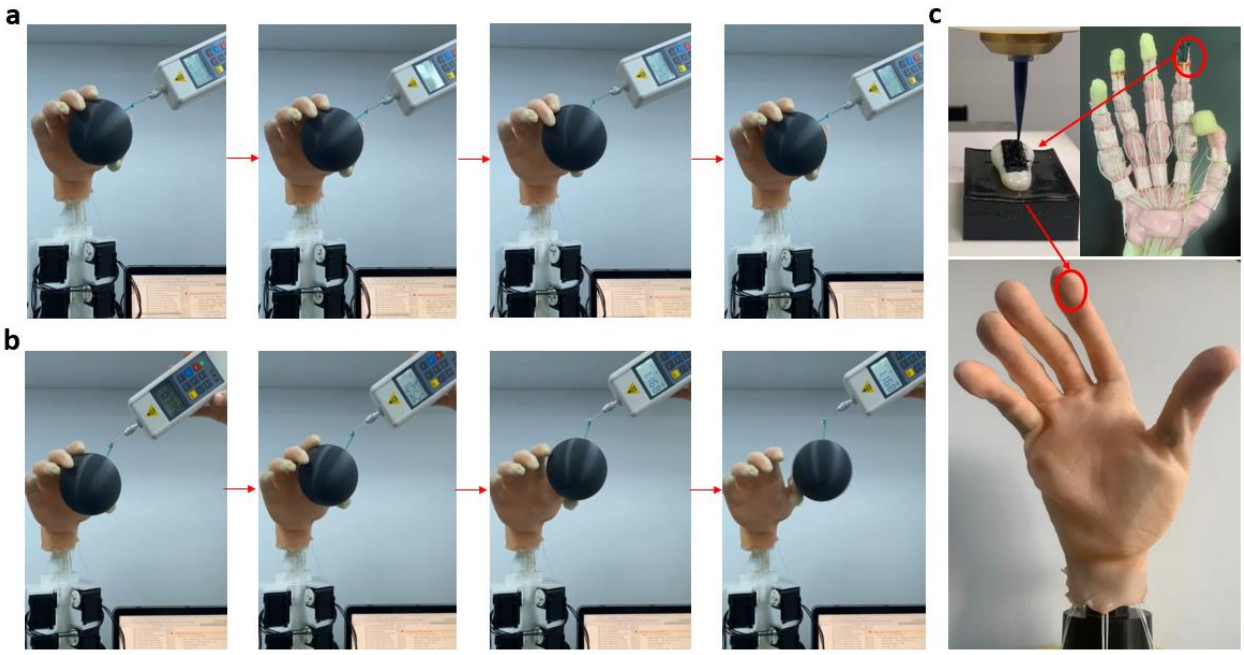

Fig.6. The closed-loop control of a biomimetic hand with tactile sensor printed on the index fingertip. (**a**) A plastic ball with diameter of 70mm was grasped by the biomimetic hand, approximately 0.75N pulling force was applied onto the ball. The biomimetic hand with tactile feedback from the sensor can sense the slip of the ball and grasp firmly. (**b**) The biomimetic hand without tactile feedback cannot produce a stable grasp. (**c**) The tactile sensor (indicated in red circle) was printed directly onto the distal phalange of index finger and then covered by the artificial skin as a biomimetic hand.

Discussion

Many tactile sensors were developed over the past decade while some of them were based on sophisticated fabricating process such as molding 7,13,18,37,38, photolithography, etching 14-17 which need high-demanding operating environment. Others employed the advanced composite material 6,9,13 resulted in a sophisticated process of material preparation. Also, the compliance between the tactile sensor

315 and its working surface was rarely considered, the tactile or pressure sensors were supposed to be used on
316 arbitrary surfaces in many cases 39,40. A high-performance and easily fabricated tactile sensor compliant
317 with uneven surface is presented in this study. This 3D printed tactile sensor is able to detect the normal
318 and shear forces with sensitivities of $2.42KPa^{-1}$and $2.26N^{-1}$ which is in line with most of the existing
319 high-performance tactile sensors 1-3,11,18. The tactile sensor proposed in this study was designed to
320 work on complex surface geometries, ensuring enhanced sensing capacity to detect direction and
321 magnitude of the stimuli, whilst being rapidly fabricated at feasible cost. The performance of our tactile
322 sensor including normal, shear sensitivity, linear sensing range and lower detection limit were compared
323 with some published sensors fabricated with similar composite material 2,3,11,18,20. As presented in Fig.
324 5a, the linear sensing range of our sensor is at least one order of magnitude superior to the sensors in the
325 literature. The normal sensitivity is also larger than the published sensors, whilst the shear sensitivity and
326 lower detection limit of this tactile sensor are in line with others.

327 The inter-locked structure was employed to mimic the biomechanical characteristics of the human skin,
328 making the structure more sensitive to the variations of strain components while enabling the sensor to
329 detect the direction of the stimuli. Meanwhile, the auxetic structure is optimized and validated against the
330 experimental results. The re-entrant angle and thickness of the sensor are the main geometrical factors
331 dominating the negative Poisson's ratio effect of the auxetic structure. These two factors were optimized
332 with the nominal sensor sensitivity and the simulation results suggested that the re-entrant angle of 65°
333 and the H/L ratio of 1.60 can provide the best piezoresistive effect. The self-contact area was significantly
334 increased by integrating the auxetic structure, leading to a wide linear sensing range. Simulation results
335 also suggested that the negative Poisson's ratio enabled a large self-contact area which was linearly
336 increased with the applied forces in the sensor with biomimetic and meta features. The sensing range
337 were significantly increased from 0.1 MPa to 0.5 MPa. Since the piezoresistive characteristics of the
338 elastic polymer-based sensor was dominated by the stress/strain related parameters during external stimuli,
339 the higher sensitivity might be caused by the sensitive SED variation to the external stimuli according to

our simulation results. The normal sensitivity was enhanced from $0.94KPa^{-1}$ to $2.42KPa^{-1}$ with the interlock and auxetic features, making the structure to be more responsive to the variation of normal pressure, then leading to a better piezoresistive performance. The shear sensitivity was doubled (from $1.58N^{-1}$ only with inter-lock features to $2.26N^{-1}$) with the optimized authentic structure whilst the lowest detection limit can reach to 10 Pa which is comparable with most of the published high-performance tactile sensors 2,3,11,18.

The sensor in this study has shown that a better performance can be achieved by integrating the auxetic or other Meta structure. The application of the optimized auxetic structure may provide new insights towards the designing of tactile sensor in the future. The tactile sensor can be fully printed directly and efficiently (rapid prototyped) onto any uneven surfaces such as the human phalange, proximal femur bones and the plateau of lumber vertebra perfectly compliant with the attached surface. Fast and simple fabrication process and the compatibility with arbitrary surfaces are critical for the future application of tactile sensor.

In summary, a fully 3D printed flexible tactile sensor based on biomimetic inter-lock and auxetic structure of CNT-Silicone rubber piezoresistive was developed for sensing the arbitrary contact force. The 3D direct writing technique was applied to print the CNT-Silicone and silver-coated powder-silicone composite directly onto the working surfaces, fabricating the tactile sensors efficiently and economically. Similar performance to most of the published high-performance tactile sensors was achieved 2,3,11,18. The integrated biomimetic and auxetic structure dominate the high sensitivity and large linear sensing range of the sensor. The auxetic structure proposed in this study can be effectively used to in the structural design of pressure sensors due to its unique mechanical properties. The sensors were rapidly fabricated onto its working surfaces like distal phalangeal bone, human vertebra and distal femur bone to monitor the sophisticated biomechanical contact or providing sensorimotor control for robotic hand. With the 3D printing technique and a simple material preparation process, the tactile sensor arrays can be

manufactured efficiently and applied to working surfaces but with a better piezoresistive performance, durability than other sensors.

Methods

Material preparation for 3D printing

The high purity (95 wt%) Multi-Walled CNT (XFM25, XFNano, China) was dispersed uniformly in isopropanol by ultrasonic dispersion at 26℃ for 6 h to obtain a good CNT suspension (Fig. 2a). The silicone main agent (Polycraft GP3481-F Silicone rubber, MB Fibreglass, UK) was added into the CNT-isopropanol suspension and was heated to 100℃ under magnetic stirring until the isopropanol was completely evaporated. After cooling down to the room temperature, the silicone curing agent was added to the composite under the weight ratio of 10:1. Our research showed that the conductivity of the CNT-silicone composite can meet the requirement of the tactile sensor with 2wt% of Multi-Walled CNT (Supplementary Fig. 4). Silver coated copper-powder-silicone composite (Fig. 3a) was used to print the electrode of the sensor. It was prepared by mixing the silver coated copper palate (48 μm) with silicone rubber with the weight ratio of 1:3.5. The coupling agent (KH550) was then added under the weight ratio of 1:100 and mechanically mixed with the composite to improve the conductivity.

Testing platform for sensor characterizations

In order to take full advantage of the piezoresistive and mechanical properties of the interlocked-auxetic features, the standard sensor with the sensing area of $2 \times 2cm^2$ consisting of 16 sensing elements was fabricated for characterization (Fig. 4). The sensor prototype was powered by 5V DC supply and connected into a customized electronic circuit. The output current was measured and collected by the multimeter (Keysight 34465A, Keysight Ltd., HK) at the frequency of 500Hz. The normal pressure applied onto the sensor was controlled by the universal testing machine (WH-5000, Weiheng Co., China) (above 10KPa) and a precise push-pull dynamometer (below 10KPa). The push-pull dynamometer was

mounted onto a horizontal tensile test platform (Supplementary Fig. 5) to produce shear force for charactering piezoresistive effects under the stimuli from horizontal directions.

The FE modelling and optimization of the sensor structure

The tactile sensors with different auxetic structures were designed and modelled in Creo Parametric (PTC Inc. Boston, US). Two key geometric parameters including the re-entrant angle (from 45° to 90° with the increment of 1°) and the H/L (Fig2.b) ratio (H/L=2.7, 2.0, 1.6 1.3 1.0) were optimized. 230 tactile sensors with different gematrical parameters were modelled for structural optimization (46 re-entrant angles together with 5 H/L ratio, resulting in 46×5 =230 different auxetic structures). The compression test was simulated in commercial FE software Abaqus. The heights of the inter-locked large and small papilla structures were adjusted with the auxetic structure as $L \times sin\theta$ (Fig. 3a) while the diameters remained constant. The goal of the optimization was to achieve the largest nominal sensitivity among the sensors with different auxetic structures. The material property for the sensors were defined as linear elastic with the Young's Modulus of 2.0MPa and Poisson's ratio of 0.3. A flat plate was modelled to compress the sensor to a specified displacement. The bottom surface of the sensor was fixed and the mesh size of 0.5mm with tetrahedral element was used for the simulation. 'Hard contact' was assigned between the flat plate and the sensor, the 'self-contact' was defined over all the external and internal surfaces of the sensor to measure the self-contact area during the compression. The strain energy density was extracted on the nodes of the surfaces defined under self-contact for deriving the nominal sensor sensitivity. In total 230 simulations with different auxetic structures were carried out for the optimization to find the largest nominal sensitivity under the same external stimuli. The simulation results were also validated against the experimental data, a good agreement was achieved between nominal and real sensitivity. Therefore, the FE simulation provided reliable optimization results of the structural design.

The bone-on-bone load monitoring and sensorimotor control of the biomimetic hand with the tactile sensor

The sensor printed onto the lumber vertebra and the distal femur head, connected with a customized circuit composed of two shift registers, two multiplexers and an Arduino Uno board for collecting the analog output from the tactile sensing elements. The analog output was converted into digital signals and visualized through the GUI programmed in Processing IDE (Processing.org). The femur, vertebra and inter-vertebra disc were 3D printed with UV curable resin as the target surfaces for printing the sensor.

A tendon-driven biomimetic hand containing intact hand bone skeleton, interphalangeal ligaments, tendon and skin was employed in this study to demonstrate the sensorimotor control with the 3D printed tactile sensor. The skeleton of the hand was 3D printed with polylactic acid (PLA) and the soft-tissues were modeled with silicone-rubber. The anthropomorphic size of the biomimetic hand was reconstructed from a 23-year-old male subject. Five electric motors (Dynamixel MX-12W, Robotics Inc., US) were used to drive the biomimetic hand, each motor is corresponded to a human forearm muscle associated with the hand grasping. The sensor was 3D printed onto the distal phalange of the index, connected with the same customized electric circuit to collect the analog output from the tactile sensing elements and convert it to digital signals as the feedback for controlling the biomimetic hand. The in-vivo grasping experiment was carried out and the muscle forces under reactive and active touch were derived based on the electromyographic signals collected by Delsys system (Delsys Trigno, Delsys Inc., US). The motors of the biomimetic hand were then modulated to obtain the similar pulling forces with human forearm muscles. A python program was developed for processing the digital signal input from the Uno board connected with the tactile sensor, applying displacement and torque control algorithm to the motors and restoring biological sensorimotor control function on biomimetic hand. Tactile signals of the biomimetic hand under sensorimotor control and active touch were obtained, enabling the human-like grasping performance of next generation prosthetics.

Data Availability

The source data including Supplementary Figures 1-7 and Supplementary Movie 1-4 are provided with this paper. The 3D printing process of the tactile sensor on a finger bone is presented in Movie 1. Movie 2

shows the FE simulations for the optimization of the auxetic structure of the sensor. Movie 3 displays the measurement of the intervertebral disc pressure and the mechanical load acting at the hip joint using the 3D printed sensor. Movie 4 presents the measurement of the finger contact pressure and sensorimotor control of a biomimetic hand based on the tactile feedback of the 3D printed sensor. The 3D model and 2D drawings of the propeosed tactile sensor can be found on figshare (https://figshare.com/articles/figure/3D_Model_and_Drawings_of_the_Tactile_Sensor_NatCom_2021/16569696). Data supporting the findings of this manuscript are available from the corresponding author upon reasonable request.

Code Availability

The G code for 3D printing the sensor and the Python code for performing sensorimotor control on biomimetic hand are available on OSF (https://osf.io/p2uyt/?view_only=d62014436e414ce69ab22f0a496033b3).

References

1 Chen, X. *et al.* Flexible three-axial tactile sensors with microstructure-enhanced piezoelectric effect and specially-arranged piezoelectric arrays. *Smart Materials and Structures* **27**, 025018 (2018).

2 Choi, E. *et al.* Highly sensitive tactile shear sensor using spatially digitized contact electrodes. *Sensors* **19**, 1300 (2019).

3 Li, X. *et al.* Highly sensitive flexible tactile sensors based on microstructured multiwall carbon nanotube arrays. *Scripta Materialia* **129**, 61-64 (2017).

4 Luo, N. *et al.* Hollow-structured graphene–silicone-composite-based piezoresistive sensors: Decoupled property tuning and bending reliability. *Advanced materials* **29**, 1702675 (2017).

5 Wang, Z. *et al.* Full 3D printing of stretchable piezoresistive sensor with hierarchical porosity and multimodulus architecture. *Advanced Functional Materials* **29**, 1807569 (2019).

6 Ha, M. *et al.* Bioinspired interlocked and hierarchical design of ZnO nanowire arrays for static and dynamic pressure-sensitive electronic skins. *Advanced Functional Materials* **25**, 2841-2849 (2015).

7 Jung, M. *et al.* Transparent and flexible Mayan-pyramid-based pressure sensor using facile-transferred indium tin oxide for bimodal sensor applications. *Scientific reports* **9**, 1-11 (2019).

8 Kwon, D. *et al.* Highly sensitive, flexible, and wearable pressure sensor based on a giant piezocapacitive effect of three-dimensional microporous elastomeric dielectric layer. *ACS applied materials & interfaces* **8**, 16922-16931 (2016).

9 Lee, Y. *et al.* Flexible ferroelectric sensors with ultrahigh pressure sensitivity and linear response over exceptionally broad pressure range. *ACS nano* **12**, 4045-4054 (2018).

10 Park, J., Kim, M., Lee, Y., Lee, H. S. & Ko, H. Fingertip skin–inspired microstructured ferroelectric skins discriminate static/dynamic pressure and temperature stimuli. *Science advances* **1**, e1500661 (2015).

11 Park, J. *et al.* Tactile-direction-sensitive and stretchable electronic skins based on human-skin-inspired interlocked microstructures. *ACS nano* **8**, 12020-12029 (2014).

12 Hasan, S. A. U. *et al.* A sensitivity enhanced MWCNT/PDMS tactile sensor using micropillars and low energy Ar+ ion beam treatment. *Sensors* **16**, 93 (2016).

13 Wang, Y., Zhu, L., Mei, D. & Zhu, W. A highly flexible tactile sensor with an interlocked truncated sawtooth structure based on stretchable graphene/silver/silicone rubber composites. *Journal of Materials Chemistry C* **7**, 8669-8679 (2019).

14 Makihata, M. *et al.* Design and fabrication technology of low profile tactile sensor with digital interface for whole body robot skin. *Sensors* **18**, 2374 (2018).

15 Oh, H., Yi, G.-C., Yip, M. & Dayeh, S. A. Scalable tactile sensor arrays on flexible substrates with high spatiotemporal resolution enabling slip and grip for closed-loop robotics. *Science advances* **6**, eabd7795 (2020).

16 Pyo, S., Lee, J.-I., Kim, M.-O., Lee, H.-K. & Kim, J. Polymer-based flexible and multi-directional tactile sensor with multiple NiCr piezoresistors. *Micro and Nano Systems Letters* **7**, 1-8 (2019).

17 Zhu, B. *et al.* Microstructured graphene arrays for highly sensitive flexible tactile sensors. *Small* **10**, 3625-3631 (2014).

18 Sun, X. *et al.* Flexible tactile electronic skin sensor with 3D force detection based on porous CNTs/PDMS nanocomposites. *Nano-Micro Letters* **11**, 57 (2019).

19 Kou, H. *et al.* Wireless wide-range pressure sensor based on graphene/PDMS sponge for tactile monitoring. *Scientific reports* **9**, 1-7 (2019).

20 Boutry, C. M. *et al.* A hierarchically patterned, bioinspired e-skin able to detect the direction of applied pressure for robotics. *Science Robotics* **3** (2018).

21 Han, Z. *et al.* Fabrication of highly pressure-sensitive, hydrophobic, and flexible 3D carbon nanofiber networks by electrospinning for human physiological signal monitoring. *Nanoscale* **11**, 5942-5950 (2019).

22 Pang, C. *et al.* A flexible and highly sensitive strain-gauge sensor using reversible interlocking of nanofibres. *Nature materials* **11**, 795-801 (2012).

23 Camilli, L. & Passacantando, M. Advances on sensors based on carbon nanotubes. *Chemosensors* **6**, 62 (2018).

24 Ma, P.-C. *et al.* Enhanced electrical conductivity of nanocomposites containing hybrid fillers of carbon nanotubes and carbon black. *ACS applied materials & interfaces* **1**, 1090-1096 (2009).

25 Obitayo, W. & Liu, T. A review: Carbon nanotube-based piezoresistive strain sensors. *Journal of Sensors* **2012** (2012).

26 Yi, Z., Zhang, Y. & Peters, J. Biomimetic tactile sensors and signal processing with spike trains: A review. *Sensors and Actuators A: Physical* **269**, 41-52 (2018).

27 Koç, İ. M. & Akça, E. Design of a piezoelectric based tactile sensor with bio-inspired micro/nano-pillars. *Tribology International* **59**, 321-331 (2013).

28 Devaraj, H. *et al.* Bio-inspired flow sensor from printed PEDOT: PSS micro-hairs. *Bioinspiration & biomimetics* **10**, 016017 (2015).

29 Wan, Y. *et al.* A Highly Sensitive Flexible Capacitive Tactile Sensor with Sparse and High-Aspect-Ratio Microstructures. *Advanced Electronic Materials* **4**, 1700586 (2018).

30 Amoli, V. *et al.* Biomimetics for high-performance flexible tactile sensors and advanced artificial sensory systems. *Journal of Materials Chemistry C* **7**, 14816-14844 (2019).

31 Johnson, K. O. The roles and functions of cutaneous mechanoreceptors. *Current opinion in neurobiology* **11**, 455-461 (2001).

32 Evans, K. E., Nkansah, M., Hutchinson, I. & Rogers, S. Molecular network design. *Nature* **353**, 124-124 (1991).

33 Kanda, Y. Piezoresistance effect of silicon. *Sensors and Actuators A: Physical* **28**, 83-91 (1991).

34 Matsuda, K., Suzuki, K., Yamamura, K. & Kanda, Y. Nonlinear piezoresistance effects in silicon. *Journal of applied physics* **73**, 1838-1847 (1993).

35 Toriyama, T., Tanimoto, Y. & Sugiyama, S. Single crystal silicon nano-wire piezoresistors for mechanical sensors. *Journal of microelectromechanical systems* **11**, 605-611 (2002).

36 Hu, F. *et al.* Gel-Based Artificial Photonic Skin to Sense a Gentle Touch by Reflection. *ACS applied materials & interfaces* **11**, 15195-15200 (2019).

37 Ji, Z. *et al.* The design and characterization of a flexible tactile sensing array for robot skin. *Sensors* **16**, 2001 (2016).

38 Kang, K., Cho, Y. & Yu, K. J. Novel nano-materials and nano-fabrication techniques for flexible electronic systems. *Micromachines* **9**, 263 (2018).

552 39 Tiwana, M. I., Redmond, S. J. & Lovell, N. H. A review of tactile sensing technologies
553 with applications in biomedical engineering. *Sensors and Actuators A: physical* **179**, 17-
554 31 (2012).
555 40 Stassi, S., Cauda, V., Canavese, G. & Pirri, C. F. Flexible tactile sensing based on
556 piezoresistive composites: A review. *Sensors* **14**, 5296-5332 (2014).

557

558 Acknowledgements

559 We would like to thank our research group members in University of Manchester and Jilin University for
560 their great support and assistant to this study. **Funding**: This research was partly supported by the project
561 of National Key R&D Program of China (No. 2018YFC2001300), the project of National Natural Science
562 Foundation of China (No. 91948302, No. 91848204, No. 52005209, and No. 51675222). **Competing**
563 **interests**: The authors declare that they have no competing interests.

Supplementary Files

This is a list of supplementary files associated with this preprint. Click to download.

- YuyangSupplementary.pdf
- Movie1.mp4
- Movie2.mp4
- Movie3.mp4
- Movie4.mp4